

Enhanced ELM Based Channel Estimation for RIS-Assisted OFDM systems with Insufficient CP and Imperfect Hardware

Chaojin Qing, *Member, IEEE*, Li Wang, Lei Dong and Jiafan Wang

Abstract—Reconfigurable intelligent surface (RIS)-assisted orthogonal frequency division multiplexing (OFDM) systems have aroused extensive research interests due to the controllable communication environment and the performance of combating multi-path interference. However, as the premise of RIS-assisted OFDM systems, the accuracy of channel estimation is severely degraded by the increased possibility of insufficient cyclic prefix (CP) produced by extra cascaded channels of RIS and the nonlinear distortion lead by imperfect hardware. To address these issues, an enhanced extreme learning machine (ELM)-based channel estimation (eELM-CE) is proposed in this letter to facilitate accurate channel estimation. Based on the model-driven mode, least square (LS) estimation is employed to highlight the initial linear features for channel estimation. Then, according to the obtained initial features, an enhanced ELM network is constructed to refine the channel estimation. In particular, we start from the perspective of guiding it to recognize the feature, and normalize the data after the network activation function to enhance the ability of identifying non-linear factors. Experiment results show that, compared with existing methods, the proposed method achieves a much lower normalized mean square error (NMSE) given insufficient CP and imperfect hardware. In addition, the simulation results indicate that the proposed method possesses robustness against the parameter variations.

Index Terms—Insufficient cyclic prefix (CP), reconfigurable intelligent surface (RIS), extreme learning machine (ELM), channel estimation, nonlinear distortion.

I. INTRODUCTION

RECONFIGURABLE intelligent surface (RIS) has been recognized as a potential technology for future sixth generation (6G) mobile communications [1], due to its promising performances in spectrum efficiency (SE), energy efficiency (EE), etc [2]. In particular, the wireless propagation environment is manipulated by changing the phase shift [3], and this characteristic is employed for “smart cities” in massive machine type communication (mMTC) [4]. To support the performance enhancement of wireless communication systems,

This work is supported in part by the Sichuan Science and Technology Program (Grant No. 2021JDR0003), the Major Special Funds of Science and Technology of Sichuan Science and Technology Plan Project (Grant No. 19ZDZX0016 /2019YFG0395), the Demonstration Project of Chengdu Major Science and Technology Application (Grant No. 2020-YF09-00048-SN), the Key Scientific Research Fund of Xihua University (Grant No. Z1120941), and the Special Funds of Industry Development of Sichuan Province (Grant No. zylf-2018-056).

C. Qing, L. Wang and L. Dong are with the School of Electrical Engineering and Electronic Information, Xihua University, Chengdu, 610039, China (E-mail: qingchj@mail.xhu.edu.cn).

J. Wang is with the Synopsys Inc., 2025 NE Cornelius Pass Rd, Hillsboro, OR 97124, USA (E-mail: jifanw@gmail.com).

e.g., the SE and EE, accurate channel estimation is the premise of RIS systems [5], [6]. However, the channel estimation in RIS-assisted wireless systems is quite challenging due to the prohibitively high pilot overhead [1], complicated cascaded channels [6] and passive surface elements [7], etc. Especially, the premise of RIS, e.g., accurate channel estimation, is suffered from multi-path interference. Given that the orthogonal frequency division multiplexing (OFDM) is good at resisting multi-path interference [8], the RIS-assisted OFDM systems are taken into account in this letter.

For RIS-assisted OFDM systems, existing researches, e.g., [2], [3], [9], [10], are studied under two assumptions. First, the cyclic prefix (CP) length in RIS-assisted OFDM systems is longer than the maximum delay spread. Second, perfect hardware is applied in the systems. However, these two assumptions are not common for practical application in RIS-assisted OFDM systems. For the first assumption, namely, the sufficient CP, challenges come from the time-varying channels and RIS-introduced extra paths. Specifically, adopting a sufficient CP to deal with time-varying scenarios may consume massive spectrum resources [11]. Given extra paths introduced by RIS, the possibility will increase that the previously indiscernible path becomes a resolvable path, and this, in turn, increases the possibility of insufficient CP [12]. Therefore, to save valuable spectrum resources, the development of receivers with insufficient CP is highly desired. In addition to the insufficient CP, imperfect hardware is usually observed in most practical RIS-assisted OFDM systems [13]. For example, high power amplifier (HPA), digital to analog converter (DAC), etc., these hardware inevitably causes nonlinear distortion in the real application scenarios. For channel estimation, the nonlinear distortion destroys the orthogonality of the training sequence and seriously degrades the estimation accuracy [14]. Therefore, previous works, e.g., [2], [3] and [6], mainly based on the previous two assumptions, could not work well in practical applications given the scenarios of insufficient CP and nonlinear distortion.

To improve the channel estimation of RIS-assisted OFDM systems affected by insufficient CP and imperfect hardware, we introduce an enhanced extreme learning machine (ELM) network. Unlike the deep learning-based methods that require complex parameter tuning and long training time [15], the proposed ELM has the advantages of fast learning speed and performance robustness. We enhance the ELM network by using hidden-layer standardization and propose an enhanced ELM-based channel estimation (eELM-CE) method for RIS-

assisted OFDM systems. Different from the common standardization method, our standardization is added before the activation function of hidden layer to ease feature acquirement for ELM's hidden layer output. In the proposed method, the imperfect hardware and the insufficient CP are modeled as a nonlinear problem and solved by exploiting the learning ability of the enhanced ELM. Generally, the proposed method can be viewed as the model-driven mode [16] integrated with the least square (LS) estimation and an enhanced ELM network, which extracts initial features and refines the following channel estimation, respectively. In contrast, [2], [3] are mainly data-driven, without the cooperation of initial features. Simulation results show that the performance of channel estimation is significantly improved by using our proposed eELM-CE method. To the best of our knowledge, this is the first work that nonlinear distortion with insufficient CP is taken into account in channel estimation for RIS-assisted OFDM systems.

The remainder of this letter is structured as follows: In Section II, the system model of RIS-assisted OFDM systems with insufficient CP and imperfect hardware is presented. The proposed method, i.e., eELM-CE is presented in Section III, and numerical results are given in Section IV. Finally, Section V concludes our work.

Notations: Boldface upper case and lower case letters denote matrix and vector respectively. $(\cdot)^T$ and $(\cdot)^\dagger$ denote the transpose and matrix pseudo-inverse, respectively. \odot is the Hadamard product. $\|\cdot\|_2$ is the Euclidean norm. \mathbf{F}_N is the normalized $N \times N$ Fourier transform matrix. $\mathbf{0}_N$ is an $N \times 1$ zero vector. $\mathbb{E}(\cdot)$ is the mathematical expectation. $\mathbb{D}(\cdot)$ represents the variance.

II. SYSTEM MODEL

We consider a RIS-assisted OFDM system, which comprises one single-antenna transmitter, one single-antenna receiver and one multi-element RIS. This system employs N subcarriers, and assumes the CP length L_{CP} is shorter than the maximum delay spread L , i.e., $L_{CP} < L$. The time-domain signal received at the receiver is given by

$$\mathbf{y} = \tilde{\mathbf{X}}_c \mathbf{h} + \mathbf{n}, \quad (1)$$

where $\tilde{\mathbf{X}}_c \in \mathbb{C}^{(N+L_{CP}+L-1) \times L}$ is a cyclic matrix formed by the transmitted data, $\mathbf{h} = [h_1, h_2, \dots, h_L]^T$ stands for the composite channel impulse response (CIR) between the receiver and transmitter, and $\mathbf{n} \in \mathbb{C}^{(N+L_{CP}+L-1) \times 1}$ denotes the circularly symmetric complex Gaussian (CSCG) distribution with zero mean and variance σ^2 . In (1), the first column of $\tilde{\mathbf{X}}_c$ is given as

$$\tilde{\mathbf{x}} = [\tilde{x}_{-L_{CP}+1}, \dots, \tilde{x}_0, \tilde{x}_1, \dots, \tilde{x}_N, \mathbf{0}_{L-1}]^T, \quad (2)$$

where \tilde{x}_i , $i = -L_{CP} + 1, \dots, N$ denotes the distorted data. That is, the transmitted data x_i experiences the nonlinear distortion caused by imperfect hardware to form \tilde{x}_i , which is expressed as

$$\tilde{x}_i = f_{\text{dis}}(x_i), \quad (3)$$

where we use the function $f_{\text{dis}}(\cdot)$ to describe the nonlinear distortion caused by imperfect hardware [15].

The composite CIR between the receiver and transmitter is represented by

$$\mathbf{h} = \mathbf{h}_{\text{TR}} + \mathbf{H}_{\text{TRR}} \phi, \quad (4)$$

where $\mathbf{h}_{\text{TR}} \in \mathbb{C}^{L \times 1}$ is the CIR of the transmitter-receiver direct link, $\mathbf{H}_{\text{TRR}} \in \mathbb{C}^{L \times M}$ is the equivalent cascaded CIR of the reflecting link, $\mathbf{H}_{\text{TRR}} = [\mathbf{h}_{\text{TRR},1}, \mathbf{h}_{\text{TRR},2}, \dots, \mathbf{h}_{\text{TRR},M}]$ is stacked by $\mathbf{h}_{\text{TRR},m}$ with $m = 1, \dots, M$, and $\phi \triangleq [\phi_1, \phi_2, \dots, \phi_M]^T$ means the phase-shift vector defined by $\phi_m = \beta_m e^{j\varphi_m}$. Similar to [6], in order to maximize the reflection power of the RIS and simplify the hardware design, we fix $\beta_m = 1$.

The equivalent cascaded CIR of the reflecting link is given by

$$\mathbf{h}_{\text{TRR},m} = \mathbf{h}_{\text{TR},m} \odot \mathbf{h}_{\text{RR},m}, \quad (5)$$

where $\mathbf{h}_{\text{TR},m} \in \mathbb{C}^{L \times 1}$ and $\mathbf{h}_{\text{RR},m} \in \mathbb{C}^{L \times 1}$ are the aggregated CIRs of the transmitter-RIS link and RIS-receiver link associated with the m -th sub-surface, respectively.

According to (1), (4) and (5), the equivalent baseband received signal in time domain is rewritten by

$$\mathbf{y} = \tilde{\mathbf{X}}_c \left(\mathbf{h}_{\text{TR}} + \sum_{m=1}^M (\mathbf{h}_{\text{TR},m} \phi_m \odot \mathbf{h}_{\text{RR},m}) \right) + \mathbf{n}. \quad (6)$$

With the received signal \mathbf{y} , we use the LS estimation to highlight the initial estimation features for easing network learning. Then, an eELM-CE method is proposed in Section III to improve the estimation accuracy for the case of insufficient CP with imperfect hardware.

III. ENHANCED ELM-BASED CHANNEL ESTIMATION

A. Estimation Preprocessing

With the received signal \mathbf{y} , we first remove its CP, and then employ LS estimation to obtain the initial features of channel estimation in the frequency domain. According to the transmission protocol proposed in [17], two OFDM blocks are transmitted in each time slot. From [17], it is assumed that the pilot tone, denoted as \mathbf{c} , and the transmitted data consist in the first and second OFDM block, respectively. Hence, we transmit $M+1$ slots due to the purpose to separate the direct link and reflecting link [6].

For LS estimation, the received pilot signal, denoted by $\mathbf{Y}_P = [\mathbf{y}_{P,1}, \mathbf{y}_{P,2}, \dots, \mathbf{y}_{P,M+1}]$, is first picked out from the received signal $\mathbf{Y} = [\mathbf{y}_1, \mathbf{y}_2, \dots, \mathbf{y}_{M+1}]$. Then, the received pilot signal \mathbf{Y}_P and transmitted pilot tone $\mathbf{C} = [\mathbf{c}_1, \mathbf{c}_2, \dots, \mathbf{c}_{M+1}]$ are respectively transformed into frequency domain by using Discrete Fourier Transform (DFT), which are expressed as

$$\begin{cases} \bar{\mathbf{Y}}_p = \mathbf{F}_N \mathbf{Y}_p \\ \bar{\mathbf{C}} = \mathbf{F}_N \mathbf{C} \end{cases}, \quad (7)$$

where $\bar{\mathbf{Y}}_p$ and $\bar{\mathbf{C}}$ represent the received pilot signal and transmitted pilot in the frequency domain, respectively. With $\bar{\mathbf{Y}}_p$ and $\bar{\mathbf{C}}$, we employ LS estimation to obtain the initial channel frequency response (CFR) of the composite channel, which is given by

Algorithm 1 eELM-CE method

Input: Separated CFRs $\widehat{\mathbf{H}} \triangleq [\widehat{\mathbf{h}}_{\text{TR}}, \widehat{\mathbf{h}}_{\text{TRR},1}, \dots, \widehat{\mathbf{h}}_{\text{TRR},M}]$.
Output: Refined CFRs $\widetilde{\mathbf{H}} \triangleq [\widetilde{\mathbf{h}}_{\text{TR}}, \widetilde{\mathbf{h}}_{\text{TRR},1}, \dots, \widetilde{\mathbf{h}}_{\text{TRR},M}]$.

Offline Training:

- 1: Initialize the weight \mathbf{W} and bias \mathbf{b} .
- 2: **for** $j = 1, \dots, M + 1$ **do**
- 3: **for** $t = 1, \dots, N_d$ **do**
- 4: Normalize the samples $\widehat{\mathbf{h}}_j^{(t)}$ using Eq. (11) to form $\widehat{\mathbf{h}}_{\text{st},j}^{(t)}$.
- 5: Calculate the output $\mathbf{o}_j^{(t)}$ of the hidden layer after $\widehat{\mathbf{h}}_{\text{st},j}^{(t)}$ through the activation function $\sigma(\cdot)$ using Eq. (12) and Eq. (13) according to \mathbf{W} and \mathbf{b} .
- 6: **end for**
- 7: Collect the output $\mathbf{O}_j = [\mathbf{o}_j^{(1)}, \dots, \mathbf{o}_j^{(N_d)}]$.
- 8: Use the known labels \mathbf{H}_j and \mathbf{O}_j to calculate the hidden layer output weight β_j using Eq. (14).
- 9: **end for**

Online Deployment:

- 10: Perform LS estimation to obtain $\overline{\mathbf{h}}_{\text{LS}}$ using Eq. (8).
- 11: Separate the CFRs of the direct link $\overline{\mathbf{h}}_{\text{TR}}$ and reflecting link $\overline{\mathbf{H}}_{\text{TRR}}$ using Eq. (9).
- 12: Use the CFRs preprocessed to form $\overline{\mathbf{H}} \triangleq [\overline{\mathbf{h}}_{\text{TR}}, \overline{\mathbf{h}}_{\text{TRR},1}, \dots, \overline{\mathbf{h}}_{\text{TRR},M}]$.
- 13: **for** $j = 1, \dots, M + 1$ **do**
- 14: Normalize $\overline{\mathbf{h}}_j$ using Eq. (11) to form $\overline{\mathbf{h}}_{\text{st},j}$.
- 15: Feed $\overline{\mathbf{h}}_{\text{st},j}$ into the trained ELM-based network using Eq. (15) to obtain the refined CFR $\widetilde{\mathbf{h}}_j$.
- 16: **end for**

$$\widehat{H}_{\text{LS}}(m, n) = \frac{\overline{Y}_p(m, n)}{C(m, n)}, m = 1, \dots, N; n = 1, \dots, M + 1 \quad (8)$$

where m represents the m -th row, n represents the n -th column and $\widehat{\mathbf{H}}_{\text{LS}}$ is the composite CFR between the receiver and transmitter. Using the transmission protocol proposed in [6], the CFRs of direct link and reflecting link are separated by

$$\begin{bmatrix} \widehat{\mathbf{h}}_{\text{TR}} & \widehat{\mathbf{H}}_{\text{TRR}} \end{bmatrix} = \widehat{\mathbf{H}}_{\text{LS}} \Theta^{-1}, \quad (9)$$

where $\widehat{\mathbf{h}}_{\text{TR}} \in \mathbb{C}^{N \times 1}$ denotes the direct-link CFR, $\widehat{\mathbf{H}}_{\text{TRR}} \in \mathbb{C}^{N \times M}$ is the reflecting-link CFR composed of M sub-surfaces reflection paths, and Θ represents the RIS reflection matrix which is a full-rank matrix [6]. From [6], Θ is described as

$$\Theta = \begin{bmatrix} 1 & 1 & \dots & 1 \\ \phi^{(1)} & \phi^{(2)} & \dots & \phi^{(M+1)} \end{bmatrix}, \quad (10)$$

where $\phi^{(i)}$ is the RIS's phase shift of the i -th pilot symbol.

Based on the initial CFRs, i.e., $\widehat{\mathbf{h}}_{\text{TR}}$ and $\widehat{\mathbf{H}}_{\text{TRR}}$, an eELM-CE is proposed in the following subsection (i.e., Section III-B) to refine the channel estimation.

B. Refining Estimation

The details of eELM-CE are presented in **Algorithm 1**. The processes of offline training and online deployment are

respectively given as follows.

1) *Offline Training:* In the training phase of ELM-based network, the main task is to learn the output weight. For ELM-based network, we need to train $M + 1$ ELM networks, and each ELM network training uses N_d samples. With extensive experiments, it is found that $N_d = 10000$ training samples show a good enough learning effect while no obvious improvement is noticed given more training samples. $\widehat{\mathbf{h}}_j^{(t)}$ represents the CFRs of the j -th ELM network, $j = 1, \dots, M + 1$, and the superscript t , $t = 1, \dots, N_d$, is the number of training sessions. We send the samples which are obtained using Eq. (9) into the network to calculate the network output and then obtain the output weight of hidden layer. In the algorithm, we obtain the samples and labels through Eq. (8) and Eq. (9), and then normalize the samples, which is expressed as

$$\widehat{\mathbf{h}}_{\text{st},j}^{(t)} = \frac{\widehat{\mathbf{h}}_j^{(t)}}{\|\widehat{\mathbf{h}}_j^{(t)}\|_2}. \quad (11)$$

It is worth noting that the standardization operation is added before the activation function, which is given by

$$\mathbf{y} = f_{\text{std}}(\mathbf{W}\widehat{\mathbf{h}}_{\text{st},j}^{(t)} + \mathbf{b}), \quad (12)$$

where $f_{\text{std}}(\cdot)$ denotes the standardization operator with $f_{\text{std}}(x) = x / (\mathbb{E}(\sqrt{\mathbb{D}(x)}))$. In this letter, we collectively refer to the normalization in (11) and the standardization operation in (12) as standardization. Then, the hidden layer output matrix $\mathbf{o}_j^{(t)}$ is expressed as

$$\mathbf{o}_j^{(t)} = \sigma(\mathbf{y}), \quad (13)$$

where $\sigma(\cdot)$ denotes the activation function such as sigmoid, hyperbolic tangent (tanh), rectified linear units (ReLU) [15]. By collecting $\mathbf{O}_j = [\mathbf{o}_j^{(1)}, \dots, \mathbf{o}_j^{(N_d)}]$, the hidden layer output weight β_j is obtained by

$$\beta_j = \mathbf{H}_j \mathbf{O}_j^\dagger. \quad (14)$$

2) *Online Deployment:* For the online deployment, the LS estimation given in Eq. (8) is first employed to obtain the initial features of composite CFRs. Then, we use Eq. (9) to separate the CFRs of direct link $\widehat{\mathbf{h}}_{\text{TR}}$ and reflecting link $\widehat{\mathbf{H}}_{\text{TRR}}$. According to the separated CFRs (e.g., $\widehat{\mathbf{h}}_{\text{TR}}$ and $\widehat{\mathbf{H}}_{\text{TRR}}$), we normalize the separated CFRs to form $\overline{\mathbf{h}}_{\text{st},j}$, i.e., $\overline{\mathbf{h}}_{\text{st},j} = \widehat{\mathbf{h}}_j / (\|\widehat{\mathbf{h}}_j\|_2)$. And then the network output $\widetilde{\mathbf{h}}_j$ is obtained by feeding $\overline{\mathbf{h}}_{\text{st},j}$ into the trained ELM-based network, which is given by

$$\widetilde{\mathbf{h}}_j = \beta_j \cdot \sigma(f_{\text{std}}(\mathbf{W}\overline{\mathbf{h}}_{\text{st},j} + \mathbf{b})). \quad (15)$$

IV. SIMULATION RESULTS AND ANALYSIS

In this section, the normalized mean square error (NMSE) is applied as the metric to compare the performance between the proposed method and the recent novel methods, i.e., [2], [3] and [6] with the considerations of insufficient CP and nonlinear distortion¹. The structure of this section is given

¹We respectively employ the same architectures of [2] and [3] for simulating their NMSEs. And the source code is available on the authors link: <https://github.com/meuseabe/deepChannelLearning4RIS>

as follows: The comparison of NMSE performance is given in Section IV-A. Then, in Section IV-B, the robustness of improvement with different parameters is discussed.

The basic parameters involved are listed below. The training sequence is Zadoff-Chu sequence [6], $L = 12$, $N = 64$, $L_{CP} = 8$, and $M = 8$. The training and testing of the proposed method are carried out on a server with Intel Xeon(R) E5-2620 CPU 2.1GHz \times 16, and the results are obtained by using MATLAB simulation on the server CPU due to the lack of a GPU solution. And the offline training takes about 13 seconds, whereas the online deployment of the proposed ELM network only needs 10 seconds. The frequency-selective Rician fading channels are considered. In this letter, we consider the effects of HPA, the nonlinear amplitude $A(x)$ and phase $\Phi(x)$ are respectively adopted from

$$A(x) = \frac{\alpha_a x}{1 + \beta_a x^2}, \Phi(x) = \frac{\alpha_\phi x^2}{1 + \beta_\phi x^2}, \quad (16)$$

where $\alpha_a = 1.96$, $\beta_a = 0.99$, $\alpha_\phi = 2.53$, and $\beta_\phi = 2.82$ are considered in the simulations.

In addition, the intensity of nonlinear distortion is measured by error vector magnitude (EVM), which is defined as

$$\text{EVM}(\%) = \sqrt{\frac{\sum_{n \in N} |\tilde{x}_n - R_n|^2}{\sum_{n \in N} |R_n|^2}}, \quad (17)$$

where \tilde{x}_n and R_n are the distorted and undistorted outputs of HPA given the same input, respectively. That is, for the same input, \tilde{x}_n and R_n are the outputs when HPA works in the saturated region and linear region, respectively. Except for the robustness analysis against EVMs, we set the basic value of EVM as 55%.

For simplicity, we use ‘‘Ref [2]’’, ‘‘Ref [3]’’, ‘‘Ref [6]’’ and ‘‘Prop’’ to denote the reference method given in [2], [3], [6] and the proposed eELM-CE method under nonlinear distortion with insufficient CP, respectively.

A. NMSE Performance Analysis

We add the nonlinear distortion and insufficient CP on the basis of [6], which fully proves the effectiveness of the proposed method in terms of the NMSE curves in Fig. 1. As shown in Fig. 1, the NMSE performance of ‘‘Ref [2]’’, ‘‘Ref [3]’’ and ‘‘Ref [6]’’ is much higher than that of ‘‘Prop’’.

It is noticed that the proposed method has similar or better NMSE performance than ‘‘Ref [2]’’, ‘‘Ref [3]’’ and ‘‘Ref [6]’’ during all SNR range. This is mainly due to the considerations of insufficient CP and the nonlinear distortion as well as the application of enhanced ELM. Besides, different from the data-driven mode adopted by ‘‘Ref [2]’’ and ‘‘Ref [3]’’, the model-driven mode is employed by ‘‘Prop’’ to exploit the advantages of both conventional algorithms and data-driven mode. In addition, since improving the ELM network is the principal task, we focus on the effectiveness of the proposed method, and the dedicated scenarios in ‘‘Ref [2]’’ and ‘‘Ref [3]’’ are not explored.

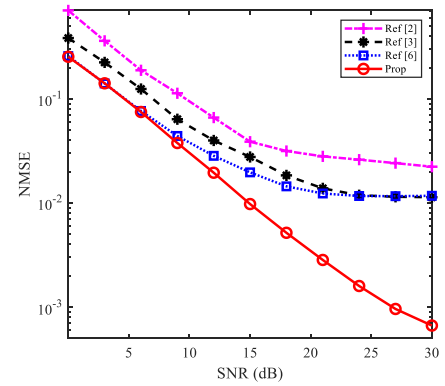


Fig. 1. NMSE vs. SNR with insufficient CP.

B. Robustness Analysis

Usually, the NMSE performance of channel estimation is influenced by the number of multi-path (i.e., L) and the degree of EVM. It is worth noting that, besides the change of the impact parameter (i.e., L and EVM), other basic parameters remain the same as those given in Section IV.

1) *Robustness against EVM*: EVM is usually used to measure the distortion intensity. To analyze the robustness of the proposed method against different distortion intensities, Fig. 2 plots the curves of NMSE with different EVMs (i.e., EVM = 45%, EVM = 55% and EVM = 65%). From Fig. 2, with the increase of EVM, the NMSEs for all curves increase due to the rise of distortion intensity. Besides, compared with ‘‘Ref [2]’’, ‘‘Ref [3]’’ and ‘‘Ref [6]’’, the ‘‘Prop’’ method achieves the smallest NMSE for each given EVM. As a result, against the impact of EVM, the ‘‘Prop’’ possesses its robustness for improving the performance of NMSE.

2) *Robustness against L* : In this paragraph, explicitly refer to Fig. 3, it can be seen from the simulations that as the degree of insufficient CP increases, the performance of the NMSE deteriorates. For example, when $L_{CP} = L - 2$, SNR = 15dB, the reference methods [2], [3] and [6] start to bend upward, but the performance is improved after using our proposed method, which reflects the robustness of our proposed method against L .

V. CONCLUSION

In this letter, a channel estimation method, eELM-CE is proposed to improve the performance of the RIS-assisted OFDM system affected by the insufficient CP and imperfect hardware. Based on the model-driven mode, LS estimation is first employed as a feature extractor to extract the initial features. Then, with the extracted initial features, an ELM network is developed to refine the channel estimation. Noteworthily, the proposed ELM networks are enhanced by using hidden-layer standardization to better capture the features of distortion and thus enhance the performance. Extensive simulation results show the effectiveness of the proposed method in relieving the influence of insufficient CP and suppressing the nonlinear distortion. The robustness of eELM-CE is also validated by its stable performance against parameter variations. In this letter, the difficulty of obtaining desired labels is simplified by

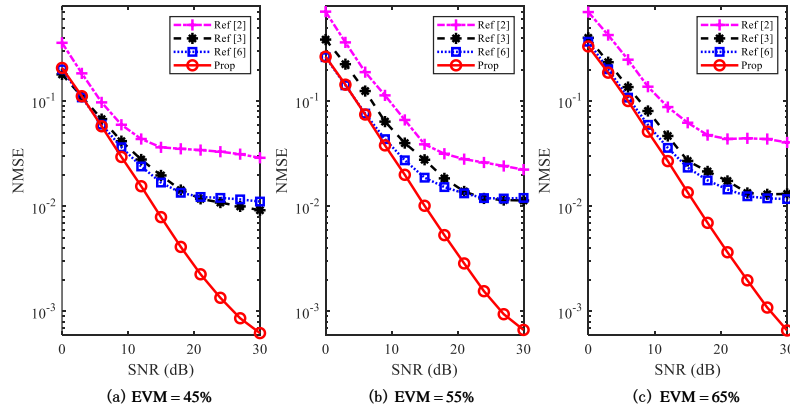


Fig. 2. NMSE vs. SNR with different EVMs.

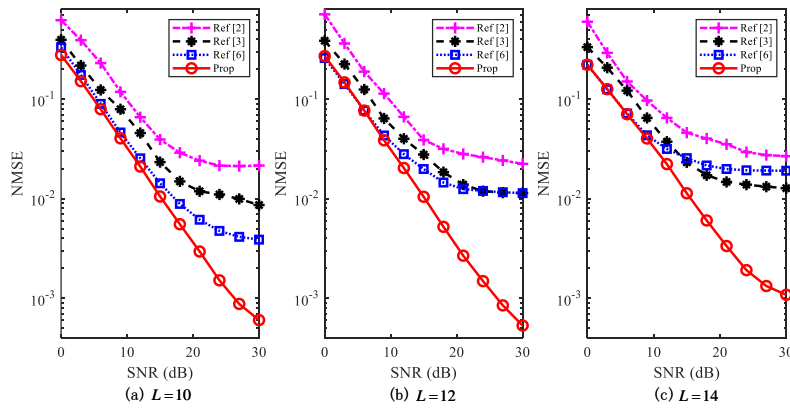


Fig. 3. NMSE vs. SNR with different numbers of multi-path L .

generating them according to the existing channel model. In our future works, we will consider the desired labels in real channel scenarios to promote the application of ELM-based channel estimation in practical systems (e.g., IoT, WLAN, etc).

REFERENCES

[1] C. Hu, L. Dai, S. Han, and X. Wang, “Two-timescale channel estimation for reconfigurable intelligent surface aided wireless communications,” *IEEE Trans. Commun.*, pp. 1–1, Apr. 2021.

[2] S. Liu, M. Lei, and M. Zhao, “Deep learning based channel estimation for intelligent reflecting surface aided MISO-OFDM systems,” in *IEEE Veh. Technol. Conf. Virtual, Victoria, BC, Canada*, Nov. 2020, pp. 1–5.

[3] A. Elbir, A. Papazafeiropoulos, P. Kourtessis, and S. Chatzinotas, “Deep channel learning for large intelligent surfaces aided mm-wave massive MIMO systems,” *IEEE Wireless Commun. Lett.*, vol. 9, no. 9, pp. 1447–1451, Sep. 2020.

[4] S. Kisseleff, W. Martins, H. Al-Hraishawi, S. Chatzinotas, and B. Ottersten, “Reconfigurable intelligent surfaces for smart cities: Research challenges and opportunities,” *IEEE open J. Commun. Soc.*, vol. 1, pp. 1781–1797, Nov. 2020.

[5] B. Zheng, C. You, and R. Zhang, “Intelligent reflecting surface assisted multi-user OFDMA: Channel estimation and training design,” *IEEE Trans. Wireless Commun.*, vol. 19, no. 12, pp. 8315–8329, Sep. 2020.

[6] B. Zheng and R. Zhang, “Intelligent reflecting surface-enhanced OFDM: Channel estimation and reflection optimization,” *IEEE Wireless Commun. Lett.*, vol. 9, no. 4, pp. 518–522, Apr. 2020.

[7] E. Shtaiwi, H. Zhang, S. Vishwanath, M. Youssef, A. Abdelhadi, and Z. Han, “Channel estimation approach for RIS assisted MIMO systems,” *IEEE Trans. Cog. Commun. and Networking*, pp. 1–1, Apr. 2021.

[8] J. Sterba and D. Kocur, “Pilot symbol aided channel estimation for OFDM system in frequency selective rayleigh fading channel,” in *Proc. Int. Conf. Radioelektronika Bratislava, Slovakia*, Jul. 2009, pp. 77–80.

[9] S. Gao, P. Dong, Z. Pan, and G. Li, “Deep multi-stage CSI acquisition for reconfigurable intelligent surface aided MIMO systems,” *IEEE Commun. Lett.*, vol. 25, no. 6, pp. 2024–2028, June 2021.

[10] Y. Wang, H. Lu, and H. Sun, “Channel estimation in IRS-enhanced mmwave system with super-resolution network,” *IEEE Commun. Lett.*, vol. 25, no. 8, pp. 2599–2603, Aug. 2021.

[11] C. Amo and M. Garcia, “Iterative joint estimation procedure for channel and frequency offset in multi-antenna OFDM systems with an insufficient cyclic prefix,” *IEEE Trans. Veh. Technol.*, vol. 62, no. 8, pp. 3653–3662, Aug. 2013.

[12] T. Jensen and E. Carvalho, “An optimal channel estimation scheme for intelligent reflecting surfaces based on a minimum variance unbiased estimator,” in *Proc. IEEE Int. Conf. Acoust. Speech Signal Process Barcelona, Spain*, May 2020, pp. 5000–5004.

[13] M. Jung, W. Saad, Y. Jang, G. Kong, and S. Choi, “Performance analysis of large intelligent surfaces (LISs): Asymptotic data rate and channel hardening effects,” *IEEE Trans. Wireless Commun.*, vol. 19, no. 3, pp. 2052–2065, Jan. 2020.

[14] D. Chi, M. Gharabally, and P. Das, “Effects of channel estimation error and nonlinear HPA on the performance of OFDM in rayleigh channels with application to 802.11n WLAN,” in *Proc. IEEE Wireless Commun. Networking Conf., Las Vegas, NV, USA*, Apr. 2008, pp. 852–857.

[15] C. Qing, W. Yu, B. Cai, J. Wang, and C. Huang, “ELM-based frame synchronization in burst-mode communication systems with nonlinear distortion,” *IEEE Wireless Commun. Lett.*, vol. 9, no. 6, pp. 915–919, Feb. 2020.

[16] J. Gao, M. Hu, C. Zhong, G. Li, and Z. Zhang, “An attention-aided deep learning framework for massive MIMO channel estimation,” *Proc. IEEE Trans. Wireless Commun.*, pp. 1–1, 2021.

[17] H. Ye, G. Li, and B. Juang, “Power of deep learning for channel estimation and signal detection in OFDM systems,” *IEEE Wireless Commun. Lett.*, vol. 7, no. 1, pp. 114–117, Feb. 2018.